ICIC Express Letters
Part B: Applications
Volume **7**, Number **3**, March **2016**

ICIC International ©2016 ISSN 2185-2766
pp. **657–664**

VIEWING-AREA SENSITIVE EOG INFLUENCES IN EEG TOPOGRAPHIC MAP THAT CONTRIBUTE TO OCULAR ARTIFACT REMOVALS IN FUTURE COMBINED ANALYSES WITH EYE-TRACKER SYSTEM

Guangyi Ai[1], Naoyuki Sato[2], Balbir Singh[1] and Hiroaki Wagatsuma[1,3]

[1]Graduate School of Life Science and Systems Engineering
Kyushu Institute of Technology
2-4 Hibikino, Wakamatsu-ku, Kitakyushu, Fukuoka 808-0196, Japan
{ ai-kouitsu; awana-balbir-singh }@edu.brain.kyutech.ac.jp; waga@brain.kyutech.ac.jp

[2]School of Systems Information Science
Future University Hakodate
116-2 Kamedanakano-cho, Hakodate, Hokkaido 041-8655, Japan
satonao@fun.ac.jp

[3]RIKEN Brain Science Institute
2-1 Hirosawa, Wako, Saitama 351-0198, Japan

Received August 2015; accepted October 2015

Abstract. *Electroencephalogram (EEG) is one of the most anticipated non-invasive methods in engineering applications to monitor brain activities in daily life, such as the brain-computer interface (BCI), to help disabled people and in the mental workload estimation in driving car to prevent human error accidents. An important issue is the contamination of ocular potentials to EEGs, known as ocular artifacts. The artifact removals are inevitable in those engineering applications. In the present study, we investigated viewing-area sensitive EOG influences in EEGs by using propagation coefficients in the regression method and topographic patterns of ICA, to maximize contributions of the eye-tracker system for the artifact removals. In the saccade task to require subjects to gaze at and pursue a target moving inside a segmented viewing-area, our experimental results demonstrated non-negligible differences in the propagation coefficients and ICA topographic patterns between three viewing conditions. Recently, high-spec eye-tracking systems are available for the simultaneous recording with EEGs. If EOG influences are significantly different depending on eye-movement directions and viewing-areas, ocular artifact removals can be done effectively by using the eye-tracker system instead of cumbersome EOG electrodes. This result extends the potential of eye-tracker systems for the ocular artifact removal in wide-range applications for daily brain activity monitoring.*
Keywords: Electroencephalogram (EEG), Electro oculogram (EOG), Artifact correction, Independent component analysis (ICA), Eye-tracker system

1. **Introduction.** Electroencephalogram (EEG) recording is a prominent non-invasive method to observe human brain activity, which has been widely used as a powerful tool not only in neuroscience studies but also in engineering areas to estimate the mental state under a specific environmental condition [1], such as brain-computer interface (BCI) helping disabled people to connect between their brain and assist devices [2,3]. The present problem is to estimate real EEG signals because EEGs are very weak in the range of microvolts and are easily contaminated by artifacts from ocular and myographic electric potentials exceeding a certain voltage level. The eye movement-related potential, which is recorded in electrooculography (EOG), is a major artifact called ocular artifact. In traditional EEG experiments, subjects are required to gaze at a fixed position on the screen to reduce the artifact [4], while it is difficult in terms of engineering applications to help daily human activities accompanied with frequent eye movements.

Ocular artifacts can be explained using spatial dipole models [5,6] to represent how electric potentials are generated with respect to cornea-retinal rotations. As for the previously-reported methods for ocular artifact removals, some methods dealt with three dimensional properties of eyeball rotations in the linear model of EEGs and EOGs [5,6], while eye movement-related EOG influences in EEGs were rarely noticed in traditional methods [7,8]. Plöchl et al. [4] introduced a combined analysis of EEG and eye-tracking data used to monitor saccade onset timings when eyeballs start to move. Recent technological advancement allows us to use a high-spec eye-tracking system with a 500Hz sampling rate close to that of the EEG recording system, leading to an effective combined analysis. EOGs can be observed directly by using electrodes attached at regular positions around eyes to achieve simultaneous recording with EEGs, while electrodes around eyes are a serious burden to experimental subjects and thus a strong restriction to engineering applications. For engineering purposes [1,2], daily-use devices with a limited number of recording channels are getting popular. If the high-speed eye-tracking system enables to pursue eye movements, EOG information could be estimated accurately from cumbersome electrodes around eyes.

How much an accurate tracking of eye movements contributes to the artifact removal is still unclear. Plöchl et al. [4] demonstrated a large offset between conditions of upward and downward saccades, which means a comparison of opposite vertical directions, whereas a comparison in horizontal saccades and an effect of saccade movement length is not clearly observed as a significant difference in the analysis of ERP topographic maps.

In the present study, we proposed a concept to complement the EOG artifact removal from EEGs with the eye-tracking system, beyond the idea of Plöchl et al. [4], and studied preliminary investigated EOG influences in the EEG topographic pattern analysis depending on viewing-area of eye movements. We hypothesized that EOG influences in the EEGs are different depending on viewing-areas, which can be called "zone-of-gaze dependency", and clearly observed the differentiations of propagation topographic patterns related to the area to gaze at and pursue visual targets. We simply designed a task to test the zone-of-gaze dependency by vertical saccade movements in different zones divided into three viewing areas horizontally.

2. **Experiment Design and Method.** In this analysis, EEG measurement data was obtained from three subjects under the following experimental conditions. All subjects sat and their heads were fixed by the head support frame (Figure 1). The head height was adjusted to the level for each subject to look at the center of the monitor screen with their eyes straightforwardly. EOG was obtained by using seven electrodes around eye (Figure 2). Visual stimulus was displayed by a 40×30cm CRT monitor with a distance of 75cm from the subject (Figure 3) and subjects were instructed to keep quiet positions to prevent the jaw and clenching artifacts. A simultaneous recording of EEGs and EOGs was monitored by 32-channel electrodes of International 10-20 System (BrainAmp amplifier, Brain Products GmbH) with the 1000Hz sampling rate. For comparison with EOGs, eye movement was obtained by a 500Hz high-speed eye-tracking system (Eyelink CL, SR Research).

2.1. **Task design.** For investigations on the zone-of-gaze dependency of EOG influences in EEG recording data, we focused on vertical saccade movements in different zones that were divided into three areas horizontally as an important step for further systematic analysis.

In the task, three zones ('left', 'middle', 'right' in Figure 4) were selected semi-randomly in every session. Individual session starts by showing a red-cross mark at the bottom position in the selected zone (a filled circle in the figure) and the subject gazes at it for 1.5s. After that, a filled red circle appears at the top position in the same zone (open circle

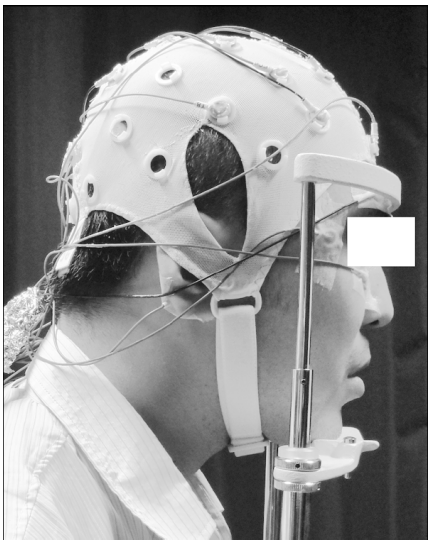

FIGURE 1. EEG channels and the head support

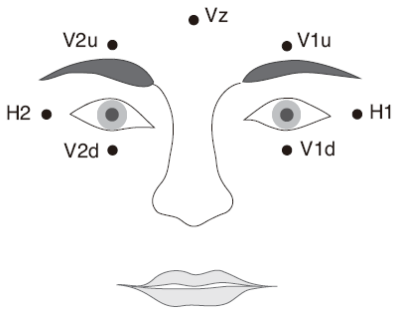

FIGURE 2. EOG electrode positions

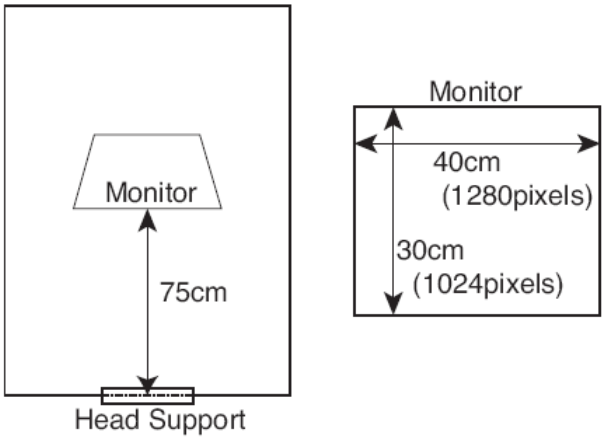

FIGURE 3. Experimental setting of the distance to the screen and its size

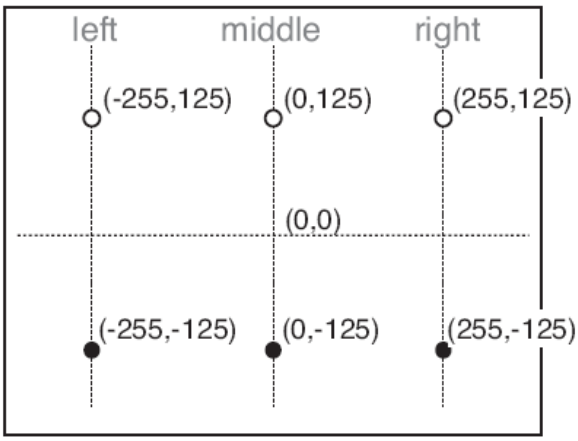

FIGURE 4. Task design with all sets of fixation positions and target positions ([pixel])

in the figure) and the appearance lasts for 1s to induce the upward saccade movement and the gaze, and then the filled circle is displaced at the bottom position and stays for 1s to induce the downward saccade and the gaze. The same protocol repeats once again. With respect to experimental setting (Figure 3), fixation and target positions in right and left zones are aligned horizontally as saccade angle from the middle, and vertical movement ranges are aligned a 12° rotation angle from the origin. Since upward and downward saccade movements are obtained two times in each session of this task, total 48 sessions including 16 sessions for each zone are performed by each subject.

2.2. **Methods for ocular artifact correction.** Various algorithms for EEG artifact removal and noise component detections have been proposed [7,9,10]. Components based algorithms have been widely used, such as principle components analysis (PCA) which decomposes multiple channel EEG signals into orthogonal components by second order statistics, and independent component analysis (ICA) which enhances the component detection by making use of higher order statistics. In ICA, non-Gaussianity or mutual information is used to decompose the EEG into equivalent number of independent components as signal channels [9,10]. Even if the computational costs were set aside the discussion, ICA component rejection has the disadvantage of having a certain amount of hands-on experience, because the rejection criterions are only empirically specified and therefore the full automation of ICA is still unsolved. In contrast, regression based methods reduce the burden by calculating EOG influences in the form of propagation coefficients based on simple statistics. After the propagation coefficients are calculated, 'real' EEG signals can be estimated from a subtraction of EOG components and multiplied by the coefficients from all EEG channels. Although the method subtracts EOG influences proportionally with less adaptiveness for temporal and spatial variations, it is still a popular method because of its simplicity [5,6,11,12], which is expected to have wide application in on-line analyses.

In the present study, we examined the zone-of-gaze dependency by using a revised regression method known as 'AAA' [11] and ICA [9,13] integrated in EEGlab [14].

2.2.1. *Regression based method.* In agreement with the previous researches [5,6,11,12], the models of EEG and EOG can be described by a linear model:

$$mEEG = rEEG + \sum_{i=1}^{M} mEOG_i \times b_i \tag{1}$$

where $mEEG$ is measured EEG signal, $rEEG$ is the 'real' EEG signal, $mEOG_i$ is the i-th EOG component, and b_i represents the propagation coefficient. The regression method by Schlögl et al. [6] assumes that EEG and EOG are independent, and then b_i can be calculated by the inner product of the inverse matrix and the auto-variance matrix of EOG signals with the cross-variance matrix between EEG and EOG signals. After the propagation coefficients are calculated, the 'real' EEG signal can be estimated by the following equation:

$$rEEG = mEEG - \sum_{i=1}^{M} mEOG_i \times b_i \tag{2}$$

where b_i represents how much EOG is transferred from eyes to the i-th channel placed over the head map, and b_i can be used to explain EOG influences as propagation patterns.

Croft and Barry [5] suggested that 3 EOG components (i.e., vertical, horizontal and radial) are necessary for EEG correction. However, vertical and horizontal EOG components are used conventionally, because of the difficulty of extracting the radial EOG [6]. Consistently, the two EOG component models were inherited by following analyses.

2.2.2. *Independent component analysis (ICA).* ICA is a well-known method for solving blind-source-separation problems. For the signals assumed as a linear combination of multiple independent components and containing up to a Gaussian signal, ICA can provide an inference of weights of components based on high order statistics. The model can be described as:

$$WA = S \tag{3}$$

where A is the only known data matrix of size number of channels-by-number of data length. S represents the source matrix which contains components no more than the number of channels in A. In most cases, whitening or sphering is done to unify the data variance through all the dimensions before solving the statistics. By maximizing the entropy or maximizing the mutual information between the inputs and the output, ICA provides an estimated un-mixing matrix with following ambiguities [9]: 1) the order of the independent components is not deterministic, and 2) the variance (in a sense of energy) of the components cannot be determined. The spatial distribution which can be obtained from the un-mixing matrix directly represents the propagation patterns. Since neuronal and non-neuronal source signals are assumed to be independent, target topographies of independent component (IC) can be selected manually based on expert knowledge. ICA was used as a preliminary analysis for extracting the propagation patterns of EOG.

3. **Experimental Result and Analysis.** Recorded data from three subjects with 144 sessions were used in this analysis, which totally contains 576 eye movements.

3.1. **EOG and eye-tracking data.** Examples of recorded EOG, eye tracking data and EEG were shown in Figure 5. The part of data for 15s demonstrated that the correlation of upward and downward movements in the vertical EOG (V-EOG) obtained by the equation of $((v1u - v1d) + (v2u - v2d))/2$ and session-to-session transitions in every 5.5s were observed in the horizontal EOG (H-EOG) by H1-H2, shifting from the middle to right and then left. The eye-tracking data (X-ETS and Y-ETS) exhibited consistent changes depending on V- and H-EOGs. With the assistance of the high-sampling rate eye-tracker system, eye movements were accurately estimated in comparison with temporal sequences of EOGs. As shown in Figure 5 (left), the eye movement pursued the visual target, which can be divided into two phases: 1) a quick saccade with a large amplitude change in 40∼60ms is observed as a long-distance jump, if the movement exceeds the target position (or to be short until the target); 2) an eye position is adjusted to reach the target position with a small amplitude change. The eye movement around 4s in the figure

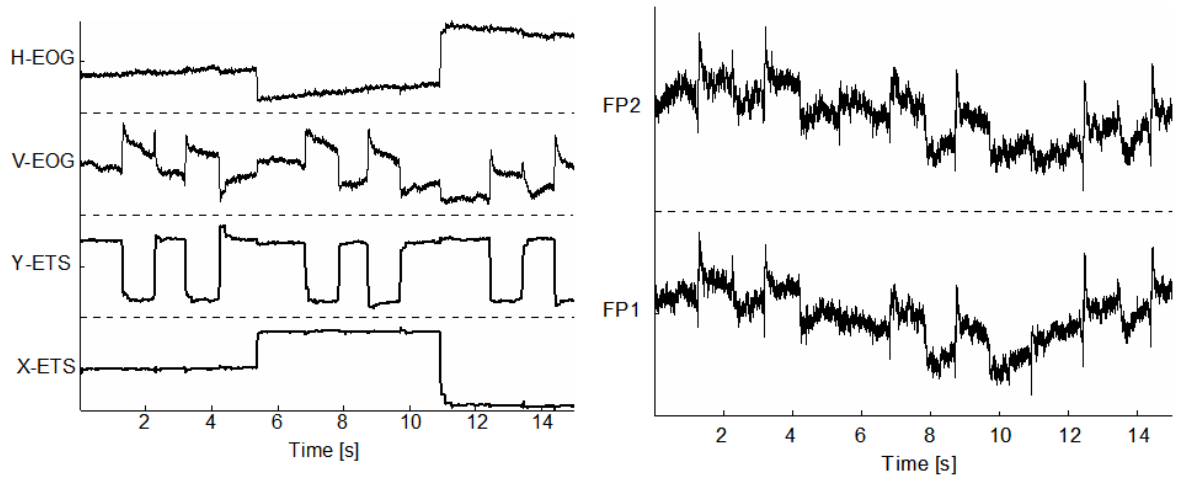

FIGURE 5. EOG, eye-tracking data and EEG raw data. Left: EOG and eye-tracking data (ETS). Right: EEG raw data from channels of FP1 and FP2.

exhibited an overrun-and-return, and movements around 10s represented a shortage-and-adjust behavior. This observation suggests that it is possible for the eye-tracking system to estimate the EOG information, which is powerful enough for artifact removals, such as linear regressions and ICA.

Figure 5 (right) showed temporal sequences of potentials in frontal EEG channels as FP1 and FP2 after band filtered with a 0.1∼30Hz FIR band pass filter. Activities in the channels were largely influenced depending on vertical EOG changes. In following sections, EOG influences depending on the viewing-area, or gaze-of-zone, were analyzed in the propagation coefficient and EEG event-related topographic maps in ICA.

3.2. **Linear regression analyses.** In the result of the regression analysis, propagation coefficients were obtained on every channel based on the procedure discussed in Section 2.2.1 and applied to the first motion of the upward saccade in every session. Resultant coefficient values of frontal channels of FP1 and FP2 were shown in Figure 6, as EEG channels expected with a large influence from EOGs. In the result, viewing-area sensitive differences were clearly observed under the left and right conditions in comparison with the middle. For all the conditions, FP2 propagation coefficients are slightly larger than FP1's, which needs further systematic analyses with multiple combinations of eye-movement directions and zones, and possibilities of bias effects of electrode positions or other asymmetric conditions in EEG channels can be considered. The difference between left and right conditions was not prominent, suggesting the comparison with topographic maps.

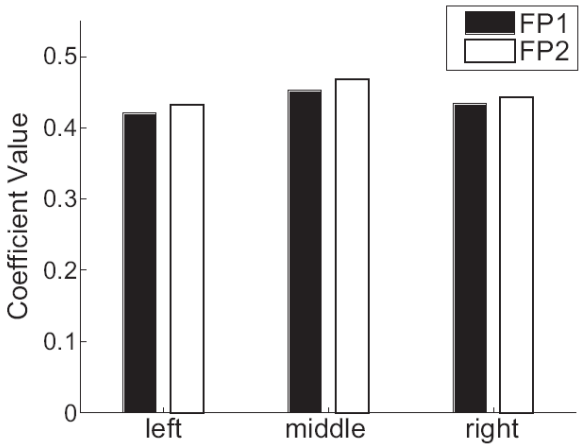

FIGURE 6. Propagation coefficients of different zones (upward saccade)

3.3. **ICA analyses.** In ICA analyses, we investigated EOG influences in EEGs after the separation of eight cases that consist of two groups (upward and downward movements) and zone-of-gaze dependency (left, middle, right, and all zone-of-gaze combination conditions). Recording data was preprocessed with a 1∼30Hz FIR band pass filter and down sampling into 500Hz to fit to the eye-tracker data. Independent components (ICs) were obtained according to the procedure shown in Section 2.2.2, and applied to each epoch defined as the period [−400ms∼600ms] with respect to the eye movement onset timing, which was defined by the time point with a maximum speed of eye-tracking data in the epoch. As an example, the topographies of EOG component were shown in Figure 7. Figure 8 showed a sample of ICs in eight epochs of the downward eye movement in the combination case. Dotted line and solid line denote epoch period and onset timing respectively.

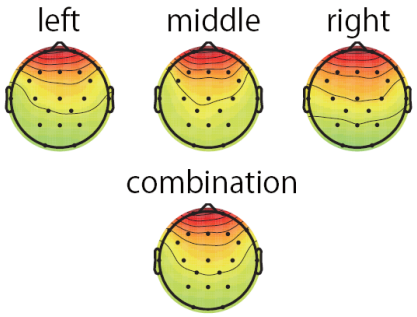

FIGURE 7. Propagation patterns from ICA depending on zone (downward saccade)

FIGURE 8. An example of ICA component decompositions (downward saccade)

Both in Figure 7 and Figure 8, the influence of zone-of-gaze dependency in EEGs appeared as differences of topographic maps in left and right conditions compared with the middle condition. In the combination case of the topographic map, a relatively smooth propagation pattern was observed with a symmetric pattern, while our zone specific analyses revealed non-negligible differences depending on the viewing area both in results of the linear regression method and ICA based topographic maps consistently. Those results indicated a risk of ignorance of the EOG zone-of-gaze dependency in EEG analyses and ocular-artifact corrections.

4. **Conclusions.** Our hypothesis of the EOG influence in EEGs in the viewpoint of zone-of-gaze dependency was preliminarily examined by the experiment with simultaneous recording of EOG, eye tracking and EEG recordings. In quantitative analyses with regression coefficient and ICA topographies, the results demonstrated a general tendency of the differences to testify the hypothesis. Our result indicates that the real eye movement analysis is important for improvements of artifact corrections by calculating the linear regression coefficients and ICA topographies separately depending on the gaze-of-zone, which have been considered as a naive assumption in traditional ocular artifact removals, yet it extends the availability of the high-spec eye-tracking system effectively. Effects of initialized positions to gaze, its range of angle and directions are considerable factors, which should be analyzed in the further investigation.

Acknowledgment. This work is partially supported by the collaborative research project with FUJITSU TEN LIMITED.

REFERENCES

[1] G. Borghini, L. Astolfi, G. Vecchiato, D. Mattia and F. Babiloni, Measuring neurophysiological signals in aircraft pilots and car drivers for the assessment of mental workload, fatigue and drowsiness, *Neuroscience & Biobehavioral Reviews*, vol.44, pp.58-75, 2012.

[2] H. Wang, Y. Li, J. Long, T. Yu and Z. Gu, An asynchronous wheelchair control by hybrid EEG-EOG brain-computer interface, *Cognitive Neurodynamics*, vol.8, no.5, pp.399-409, 2014.

[3] J. M. Henderson, S. G. Luke, J. Schmidt and J. E. Richards, Co-registration of eye movements and event-related potentials in connected-text paragraph reading, *Frontiers in Systems Neuroscience*, vol.7, 2013.

[4] M. Plöchl, J. P. Ossandón and P. König, Combining EEG and eye tracking: Identification, characterization, and correction of eye movement artifacts in electroencephalographic data, *Frontiers in Human Neuroscience*, vol.6, pp.1-23, 2012.

[5] R. J. Croft and R. J. Barry, Removal of ocular artifact from the EEG: A review, *Neurophysiologie Clinique/Clinical Neurophysiology*, vol.30, no.1, pp.5-19, 2000.

[6] A. Schlögl, C. Keinrath, D. Zimmermann, R. Scherer, R. Leeb and G. Pfurtscheller, A fully automated correction method of EOG artifacts in EEG recordings, *Clinical Neurophysiology*, vol.118, no.1, pp.98-104, 2007.

[7] J. A. Urigüen and B. Garcia-Zapirain, EEG artifact removal – State-of-the-art and guidelines, *Journal of Neural Engineering*, vol.12, no.3, pp.1-23, 2015.

[8] P. He, G. Wilson and C. Russell, Removal of ocular artifacts from electro-encephalogram by adaptive filtering, *Medical and Biological Engineering and Computing*, vol.42, no.3, pp.407-412, 2004.

[9] A. Hyvärinen, Fast and robust fixed-point algorithms for independent component analysis, *IEEE Trans. Neural Networks*, vol.10, no.3, pp.626-634, 1999.

[10] T. P. Jung, S. Makeig, C. Humphries, T. W. Lee, M. J. McKeown, V. Iragui and T. J. Sejnowski, Removing electroencephalographic artifacts by blind source separation, *Psychophysiology*, vol.37, no.2, pp.163-178, 2000.

[11] R. J. Croft and R. J. Barry, EOG correction: A new aligned-artifact average solution, *Electroencephalography and Clinical Neurophysiology*, vol.107, no.6, pp.395-401, 1998.

[12] G. Wallstrom, J. Liebner and R. E. Kass, An implementation of Bayesian adaptive regression splines (BARS) in C with S and R wrappers, *Journal of Statistical Software*, vol.26, no.1, pp.1-21, 2008.

[13] S. Makeig and J. Onton, EEG dynamics: An ICA perspective, *Oxford Handbook Event-Related Potentials*, vol.3, pp.1-51, 2011.

[14] A. Delorme and S. Makeig, EEGLAB: An open source toolbox for analysis of single-trial EEG dynamics including independent component analysis, *Journal of Neuroscience Methods*, vol.134, no.1, pp.9-21, 2004.